Decameter thick remnant glacial ice deposits on Mars

Susan J. Conway, Matthew Balme

AGU PUBLICATIONS

Geophysical Research Letters

RESEARCH LETTER
10.1002/2014GL060314

Key Points:
- Terrain-draping, latitude-dependant mantle (LDM) deposits are >46% vol. ice
- Our data show that LDM is up to 30 m thick, doubling the global inventory of ice in the LDM
- LDM is "ice sheet" like melt of LDM similar to terrestrial ice-cored moraines

Supporting Information:
- Readme
- Table S1
- Table S2
- Text S1
- Figure S1
- Figure S2

Correspondence to:
S. J. Conway,
susan.conway@open.ac.uk

Citation:
Conway, S. J., and M. R. Balme (2014), Decameter thick remnant glacial ice deposits on Mars, *Geophys. Res. Lett.*, *41*, 5402–5409, doi:10.1002/2014GL060314.

Received 23 APR 2014
Accepted 23 JUN 2014
Accepted article online 26 JUN 2014
Published online 7 AUG 2014

Decameter thick remnant glacial ice deposits on Mars

Susan J. Conway[1] and Matthew R. Balme[1,2]

[1]Department of Physical Sciences, Open University, Milton Keynes, UK, [2]Planetary Science Institute, Tucson, Arizona, USA

Abstract On Mars, a smooth, draping unit—the "latitude-dependant mantle" (LDM), believed to comprise meter thick layers of dust and ice—extends from the midlatitudes to the poles, covering at least 23% of the surface. We show that the LDM can be 30 m deep on pole-facing crater walls, and by measuring the erosional and depositional volumes of small gullies that incise these LDM deposits, we show that it must contain between 46% and 95% ice by volume. Extrapolating to a global scale, these deposits account for ~10^4 km^3 of near-surface ice, doubling previous LDM volume estimates. Thick LDM deposits can be emplaced during the many orbital variation-driven climate excursions that occurred during the Amazonian period. We suggest that LDM deposits are similar to ice sheets composed of massive ice with a surface lag.

1. Introduction

Outside the polar regions, the bulk of Mars' shallow ground ice is thought to reside within the "latitude-dependent mantle" (LDM), a morphological unit that drapes the underlying terrain [*Head et al.*, 2003; *Kreslavsky and Head*, 2000; *Mustard et al.*, 2001]. The LDM has been linked to observations of present-day, massive ground ice in the upper tens of centimeters of Mars' surface by gamma ray spectrometry remote sensing [*Feldman et al.*, 2004] and by identification of high albedo, swiftly fading deposits within newly formed impact craters at 42–56°N [*Byrne et al.*, 2009]. Shallow ice was identified in situ by the Phoenix lander at 68°N [*Smith et al.*, 2009].

The LDM covers 23% of the planet to an estimated thickness of 6–12 m at latitudes >45° in both hemispheres [*Kreslavsky and Head*, 2002]. It is interpreted to be a mixture of ice and dust based on the presence of thermal contraction polygons and sublimation-like degradation pits and on increased levels of degradation/dissection toward the midlatitudes [*Mustard et al.*, 2001; *Schon et al.*, 2012]. Impact crater size-frequency statistics show that the LDM is young (0.1–1 Ma) [*Schon et al.*, 2012] and in places comprises at least six layers [*Schon et al.*, 2009a].

On cold pole-facing slopes in the midlatitudes, the LDM often blankets the middle and lower parts, infilling local hollows, and has a well-defined, lobate margin near the top of the slope [*Christensen*, 2003]. Erosional gullies [*Malin and Edgett*, 2000] (Figure 1a) occur in such LDM deposits, inspiring suggestions that it is analogous to a "pasted-on" snowpack [*Christensen*, 2003]. Such gully-LDM systems have been previously described [*Levy et al.*, 2009b, 2011; *Schon and Head*, 2011; *Raack et al.*, 2012], and the LDM in such regions exhibits polygonal patterns associated with thermal contraction, crevasse-like fractures, downslope lineations, and steep gully incisions. This pasted-on LDM overlies other putatively ice-rich deposits, such as concentric crater fill [*Levy et al.*, 2009a]. For four sites that share these distinguishing characteristics (see supporting information for site descriptions), we used gullies to investigate the composition of the LDM by comparing the volumes of their source alcoves and terminal deposits.

2. Approach

2.1. Volume Calculations

For our volume calculations, we used ~1 m/pixel digital elevation models (DEMs) derived from stereo images acquired by the High Resolution Science Imaging Experiment (HiRISE) on board the NASA Mars Reconnaissance Orbiter (MRO). All the DEMs were produced using the software packages ISIS3 and SocetSet following the workflow of *Kirk et al.* [2008] (Table 1). The specific gullies within the LDM were chosen (i) to be widely distributed in longitude to avoid local effects (Table 1), (ii) to be morphologically representative of this type of gully [*Aston et al.*, 2011], and (iii) to have reliable stereo HiRISE coverage. We first defined a palaeotopographic surface by fitting a smooth surface to areas adjacent to, but outside of, the gully system.

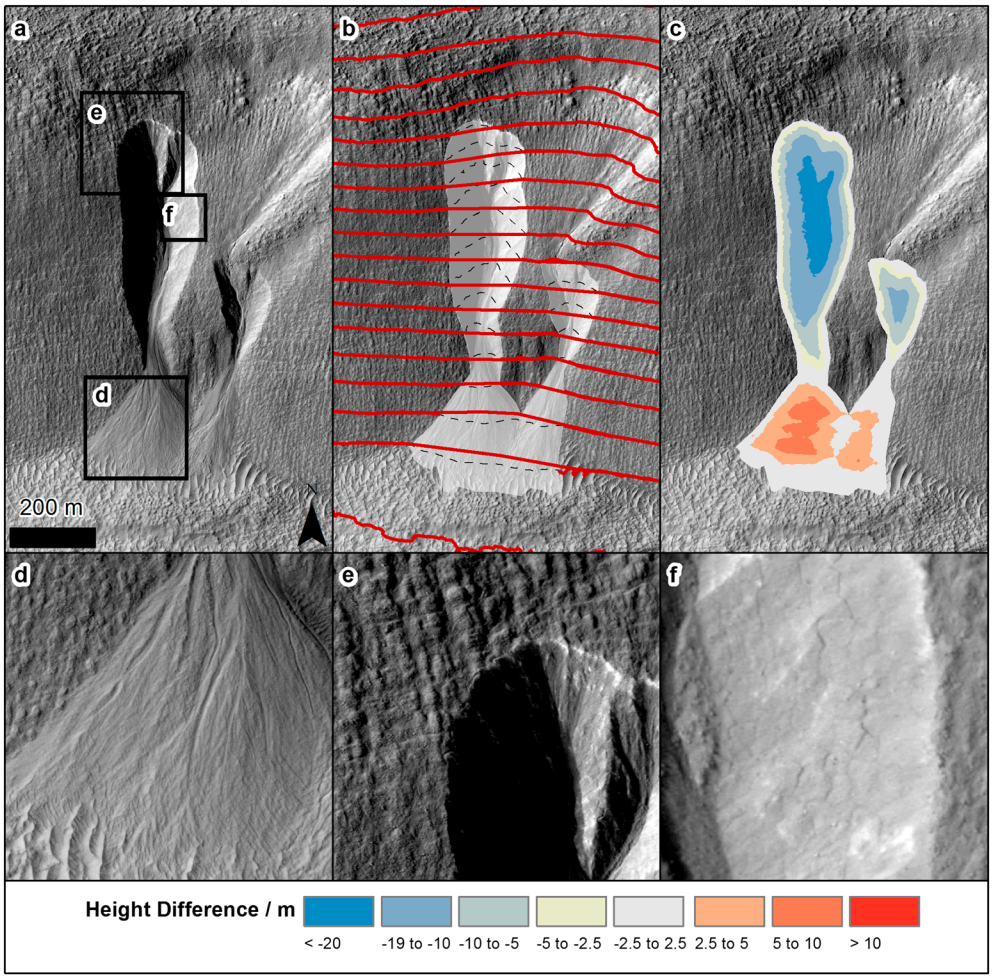

Figure 1. Example of gullies in site 3. (a) Overview of the system. (b) Same overview with 25 m extrapolated contours overlain with solid lines, the original contours as dashed lines, and the gully zone masked in white. (c) Difference map: erosion indicated by negative values, deposition by positive ones. (d) Debris apron with well-defined channels visible. (e) Gully alcove delineated by a sharp scarp which crosscuts preexisting slope lineations with no noticeable deformation. (f) Polygonal fractures on the illuminated alcove wall. The locations of Figures 1d–1f are found in Figure 1a and marked by boxes. HiRISE image PSP_002514_1420, credit NASA/JPL/UofA.

We assumed that the LDM was originally continuous because (i) the gully-adjacent regions are smooth; (ii) gullies cut preexisting textures, suggesting removal of material (Figure 1); and (iii) sharp slope breaks mark the edge of the alcoves (Figure 1e), suggesting little or no draping by mantling material postgully formation. To further constrain the palaeotopographic surface, we extended topographic contours across the gullies, which were contiguous with the undisturbed LDM on either side (Figures 1a–1c). On the depositional fans, we used 5 m contours and elsewhere 25 m contours. The palaeotopographic surface was derived by performing a natural neighbor interpolation using the gully-adjacent topography and the extrapolated contours as input data. The output was a new elevation model with the same resolution as the underlying DEM. To calculate the erosional and depositional volumes of gully material, we calculated the volume differences between the original DEM and the palaeotopographic surface. Error propagation calculations suggest that our estimates of volumes are accurate to within ~25% (section 2.2; Table 2). The maximum depth of erosion and deposition was taken as the maximum negative and positive vertical differences between the DEM and the palaeotopographic surface. We assumed that the maximum erosion depth corresponds to the maximum thickness of the removed material.

2.2. Errors in Elevation Data and Calculations

Using the method of *Okubo* [2010], we estimated the vertical precision of the DEMs to be between 0.18 m and 0.44 m (Table 1). The absolute values of the elevation were tied to Mars Orbiter Laser Altimeter point data.

Table 1. List of Data Sources for Elevation Data Used in This Study[a]

Site ID	LDM Covered Area (km^3)	HiRISE Image 1	Pixel Scale Image 1 (cm)	HiRISE Image 2	Pixel Scale Image 2 (cm)	Credit for DTM	Center Latitude	Centre Longitude	Convergence Angle (°)	Vertical Error (m)
1	1.6	ESP_012991_1335	25.1	ESP_013624_1335	25.9	University of Arizona	−45.9	9.54	9.6	0.31
2	1.5	ESP_013639_1415	25.4	ESP_013850_1415	25.5	University of Arizona	−38.1	317.3	9.7	0.30
3	36.0	PSP_002514_1420	25.4	PSP_002659_1420	25.7	Open University	−37.872	217.924	6.7	0.44
4	7.8	ESP_011672_1395	25.5	ESP_011817_1395	25.6	Open University	−40.344	20.117	15.8	0.18
5	n/a	ESP_019438_2340	30.9	ESP_027231_2340	31.8	Open University	53.554	26.313	9.1	0.40

[a]DEMs from the University of Arizona were downloaded from the HiRISE team's website and are archived on the Planetary Data System.

The error in the volume calculations is dominated by the uncertainty in deriving the palaeotopographic surface rather than noise or uncertainty in the DEM. Because we used the LDM outside of the gully systems to constrain this surface, the natural variability of the surrounding terrain is a major source of uncertainty. In order to estimate reasonable bounds for this uncertainty, we quantified the topographic variability of the terrain surrounding the gullies by measuring the deviation of its contours from a straight line on length scales of 25, 50, and 100 m. These different length scales were used because we recognized that uncertainty increases with distance. We divided the 25 m contours at each site into segments of these lengths and then measured the maximum horizontal distance between the contour and a straight line joining the ends of the segments. We performed a linear fit between the mean of these maxima and the length over which they were evaluated to produce a function describing the expected maximum deviation from a straight line over a given horizontal distance. We used this function to deflect the extrapolated contours that were used to constrain the palaeotopographic surface in both upslope and downslope directions, and then we recalculated the volumes, thus creating estimates of the uncertainty in volume and thickness (Table 2). The erosion volume error ranges from 7 to 22% (median 15%) and the deposition volume error from 9 to 86% (median 23%). The deposition error is larger because the absolute deposition volumes are smaller than the erosion volumes.

3. Gully Erosion and Deposition Volumes

We find that the volumes of the gully terminal deposits are small compared to the volumes of the depressions from which the material has been removed (Table 2). The eroded volume exceeds the deposition volume by a factor of 5.5 to 17 (Figure 2 and Table 2) in the LDM gullies studied. In contrast, the eroded and depositional volumes are equal for a gully formed in scree and bedrock (site 5; Table 2) outside of the LDM. Similarly, in closed-system gullies on Earth, erosion volumes are balanced by deposition volumes [*Bremer and Sass*, 2012]. Within the LDM on Mars, therefore, substantial volume losses must have occurred.

This LDM-specific behavior can be explained only by a loss of material after or during erosion, or if the original preerosion material had extremely high porosity, such that the compaction of the terminal deposits was much greater than the preeroded material. We reject the "high initial porosity" hypothesis: the pasted-on material supports slopes ≥30° (the angle of repose) so it cannot be a loose, dry material. Similarly, open block work slope deposits cannot express thermal contraction polygons, and volcanic deposits are unlikely to be so localized.

We think that there are only two likely explanations for this postdepositional volume loss, removal by wind or removal of a volatile substance during or after erosion. From our volume calculations, we can estimate the vertical aeolian deflation required to produce the volume imbalance. If we assume that the initial material was dry with a porosity of 30% and that the sediments are fully compacted on deposition, we calculate that these fans would have to have vertically deflated by 6.7 m on average (ranging from 0.9 to 25.5 m) to account for the volume imbalance that we observe. However, meter deep channels are preserved on the terminal debris aprons and fans (Figure 1d), arguing against substantial aeolian deflation.

Table 2. Summary of Measured Parameters and Associated Errors Per Gully System at Each Study Site

Site	Gully ID	Erosion Volume (m^3)	Erosion Error (m^3)	Deposition Volume (m^3)	Deposition Error (m^3)	Erosion / Deposition	Fraction "Missing" Material	Error in Fraction of Missing Material	Thickness of Eroded Material (m)	Error in Thickness (m)
1	0	15,8093	34,861	68,747	16,970	2.30	0.57	0.16	7.6	0.8
2	0	66,165	7,375	6,814	5,486	9.71	0.90	0.15	10.0	0.6
3	0	117,363	15,196	46,093	10,354	2.55	0.61	0.10	12.3	1.3
3	1	980,584	100,568	136,050	31,244	7.21	0.86	0.12	26.8	2.6
3	2	683,561	113,995	139,692	26,976	4.89	0.80	0.17	23.6	2.7
3	3	541,306	93,911	155,519	14,634	3.48	0.71	0.16	15.6	1.3
3	4	128,8451	233,413	401,680	99,011	3.21	0.69	0.16	29.7	3.2
3	5	248,178	43,719	43,601	12,894	5.69	0.82	0.19	13.6	2.2
3	6	45,468	3,289	24,417	3,756	1.86	0.46	0.05	8.0	0.7
3	7	824,925	93,836	168,438	29,798	4.90	0.80	0.12	24.3	2.3
3	8	12,247	1,012	4,574	671	2.68	0.63	0.07	4.7	0.2
3	9	945,939	136,715	282,514	56,911	3.35	0.70	0.13	23.1	2.4
4	0	646,071	134,690	106,247	59,924	6.08	0.84	0.24	18.6	2.0
4	1	637,544	129,052	37,506	32,424	17.00	0.94	0.27	21.1	1.0
4	2	259,370	40,487	33,869	13,531	7.66	0.87	0.19	14.4	1.1
5	0	1,168,778	55,7493	1,486,078	462,516	0.79	−0.27	0.15	26.2	8.3
Mean		497,018		110,384		5.50	0.75		16.9	
Max		1,288,451		401,680		17.00	0.94		29.7	
Min		12,247		4,574		1.86	0.46		4.7	

For sites 1 and 2, the calculated aeolian deflation is ~1.5 m, and site 1 does show evidence for aeolian activity in the form of ripples (<2 m wavelength), so we cannot rule out deflation completely in these cases. At the other two sites, aeolian bedforms are present, but we still observe ~1 m deep channels and equivalent vertical deflations of >7 m in the majority of the cases. These large aeolian deflation values are unrealistic, given the preservation of multiple generations of channels on the fans (Figure S2 in the supporting information). In the following calculations, therefore, we neglect aeolian deflation and assume that the "lost" volume of material is due to the removal of a volatile component, which in the absence of plausible alternatives, was almost certainly water ice that sublimated, or melted and then drained away, during gully emplacement.

By examining the ratio of deposited to eroded volumes in these gullies, the initial ice content of the pasted on material can be calculated from the volume of lost material. In the areas we have examined, the LDM incised by gullies contains 46–94% (mean 75%) ice by volume (Figure 2 and Table 2). This value is likely to be even higher: nine of the fifteen gullies studied are connected to upslope areas without LDM (e.g., Figure 3a) that could have contributed additional debris to the terminal deposit, hence decreasing the measured eroded/deposited volume ratio. We assume that the compaction of the solid fraction on deposition is limited, because it is uncertain if this solid fraction is derived from a surface lag, debris within the ice, or material underlying the ice; hence, its initial porosity and compressibility are unconstrained.

On the pole-facing crater slopes studied, the LDM is 5–30 m thick (mean 17 m) based on our DEM measurements (Figure 2 and Table 2)—deeper than previous LDM estimates from flatter areas at similar latitudes, which are on the order of several meters [*Mustard et al.*, 2001; *Head et al.*, 2003]. Multiple layers of LDM exist outside the impact craters at these latitudes [*Schon et al.*,

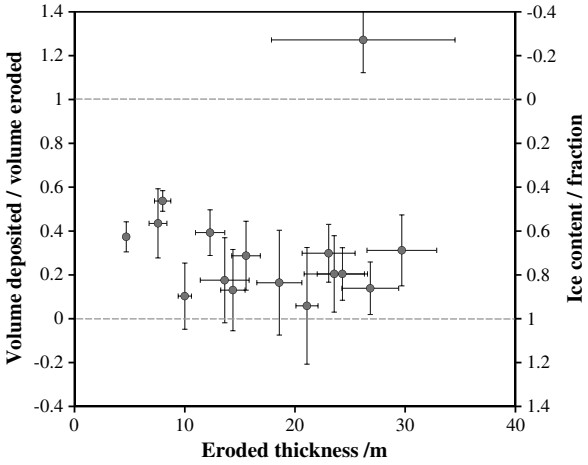

Figure 2. Ratio of (left axis) volume deposited to volume eroded and (right axis) estimated ice content plotted against the estimated thickness of LDM for 16 gullies. The anomalous point (top of plot) is a gully outside of the LDM (i.e., ice content can be ignored). The dotted lines show values <1, where erosion exceeds deposition and values >1, where deposition exceeds erosion. The error in ice content was calculated by propagating error in the contour extrapolation method.

2009a], but we have not identified layering even in freshly exposed sections (Figures 3b and 3c), suggesting that this is a single, thick layer of LDM perhaps produced in a single event. Alternatively, if successive layers have similar ice contents, multiple layers may appear as one, although development of any surface lag would inhibit this.

4. Global Extrapolation of Ice Volume

LDM deposits similar to those reported cover many pole-facing slopes at this latitude [e.g., *Levy et al.*, 2009b; *Raack et al.*, 2012]. To estimate the global inventory of ice contained in such deposits, we undertook a survey of craters between 1 and 50 km in diameter to determine (i) the frequency of such deposits and (ii) their spatial extent (in terms percent of perimeter and radius occupied).

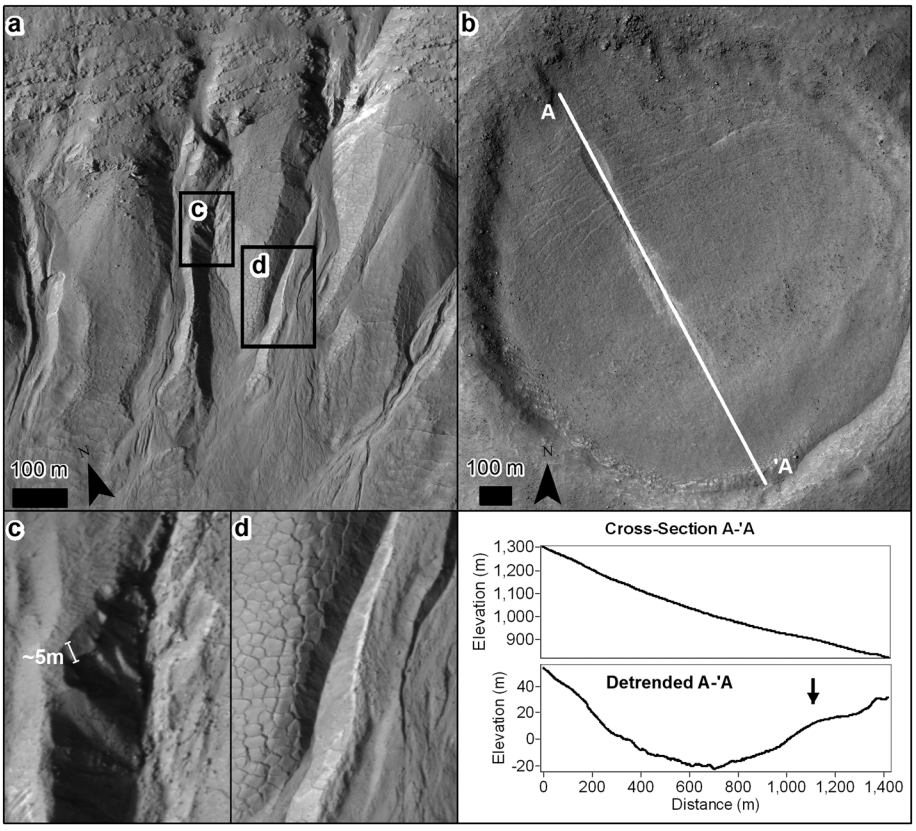

Figure 3. The gullies and the LDM. (a) "Pristine" gullies in LDM at site 4. (b) Isolated gully in LDM-filled crater at site 2, deformation of the LDM shown by crevasse-like cracks near A and a bulge at the base near 'A (arrow in detrended topographic profile). (c) Detail of gully wall; a competent layer is visible ~5 m below the undisturbed LDM surface. (d) Disintegration of LDM polygons into loose material on the gully walls; no layering is visible. The boxes in Figure 3a outline the locations of Figures 3c and 3d. HiRISE images ESP_011672_1395 (Figures 3a, 3c, and 3d) ESP_013850_1415 (Figure 3b), credit NASA/JPL/UofA.

Conway and Mangold [2013] found that pole-facing smooth deposits occur between 33 and 45°S in their survey of ice deposits in the Terra Cimmeria region. Equatorward of this zone, they found ice-free regions; poleward, smooth deposits are found in all craters covering all slope exposures. We therefore constrained our survey to latitudes 33–45° north and south. We randomly chose 200 craters from the *Robbins and Hyneck*'s [2012] crater database, and using MRO Context Camera (CTX) images, noted the presence or absence of pasted-on LDM deposits in each crater and measured the radial width and span of the perimeter occupied by any observed deposit. Table S1 in the supporting information summarizes the results of this survey. Out of the 200 craters, 44 are not covered by or had poor quality CTX data, and only 22 contain no deposits. We found little variation in the percentage of craters containing deposits with crater diameter; hence, we used the value for all craters of 87% for further calculations. The fraction of the perimeter occupied by the deposits ranges between 0 and 100%, but its mean value does not vary with crater diameter; hence, we took the mean perimeter occupation fraction of 40% as being representative of the population. We found a systematic variation in radial width of the deposit (w) with crater diameter, from $0.4 \times D$ (D = crater diameter) for craters 1-2 km in diameter to 0.1 for craters >5 km in diameter. To estimate the likely deposit width for any given crater diameter, we performed a linear least squares fit of log$D$ against w:D, thus producing a function describing how radial width changes with crater diameter.

To extrapolate these results to the global data set, we extracted all the craters <50 km in diameter from the impact crater database of *Robbins and Hynek* [2012] for latitudes between 45° and 33° north and south (excluding the Hellas Basin, Argyre Basin, and Thaumasia regions). We set the probability of a crater having LDM deposits to 0.87; the proportion of the perimeter occupied to 0.4 and calculated the radial width of the deposit as a function of the crater's diameter. At latitudes poleward of 45°, all crater walls have LDM deposits, irrespective of size, so the probability of crater having a deposit and the proportion of the perimeter occupied were both 1, with the radial width of the deposit remaining a function of the crater's diameter. We assumed an LDM thickness of 10–30 m. Multiplying these factors gave a volume of 9300–27,800 km^3 (~10^4 km^3) for the southern hemisphere. Including the northern hemisphere takes the estimate to 11 900–35,800 (~10^4 km^3). We consider this as a conservative estimate, because we do not include craters <1 km, crater rim exterior slopes, noncrater-related slopes, or the fact that LDM near the poles may be thicker. Even so, this doubles previous global estimates of the volume of ice contained within the LDM [*Mustard et al*., 2001; *Kreslavsky and Head*, 2002].

5. Discussion

5.1. Origin of the LDM

Our observations and results allow formation hypotheses for ice in the LDM to be tested. Two main hypotheses exist: slow vapor diffusion of water vapor into a regolith to form an ice-rich, particulate substrate [*Mellon and Jakosky*, 1995] or direct emplacement of ice as snow/frost accumulation [*Mustard et al*., 2001; *Head et al*., 2003; *Milliken et al*., 2003; *Schon et al*., 2009a] or frozen liquid water [*Soare et al*., 2011]. Vapor diffusion alone cannot usually produce ice volumes exceeding regolith pore space ("massive ice, usually $>$20% by volume), but recent studies of vapor transport into porous regoliths containing thermal contraction cracks [*Fisher*, 2005] show that massive ice can reach 70% by volume through diffusion processes, but only to the depths to which the cracks penetrate. Over half of our sites have both estimated ice contents of greater than 70% and polygonal fracture patterns on the surface. However, polygon spacing is always <10 m (e.g., Figures 2f, 3c, and Figure S1 in the supporting information), suggesting crack depths of only a few meters [*Lachenbruch*, 1961]. We conclude that vapor diffusion is unlikely to have emplaced such deep ice-rich deposits.

Alternative formation mechanisms to vapor diffusion include emplacement by snow or frost accumulation [*Schon et al*., 2009a], or by concentration of ice through freeze thaw cycling, as is common on Earth [*Soare et al*., 2011]. In both models, ice is protected from ongoing sublimation by a surface lag of at least several centimeters thick, derived from material liberated from within the ice during deflation, or from fallen debris. This matches observations made at the Phoenix Lander site [*Smith et al*., 2009], where massive ice was found beneath several centimeters of dry soil. If such a lag was present on intracrater LDM deposits incised by gullies, the lag material would contribute to the sediment volumes deposited at the gully terminus. If the ice content of the LDM was at the upper end of our estimated values, 94%, then we calculate that this lag would be between 0.25 and 8.24 m thick (mean 3.21 m) for our study sites. Indeed, we have observed

a mechanically resistant layer of 3 to 7 m thick (as little as 0.5 m, where polygon tops are collapsing; Figure 3c) in two fresh, steep scarps cut into the LDM (Figures 3a–3c), which we interpret to represent the top of the ground ice. The presence of a lag of this thickness both supports the accumulation model for LDM formation and is consistent with an ice content of the LDM at the upper end of our estimated range of 46–94%.

5.2. Implications for the Generation of Liquid Water

Given the high ice content of the substrate and the presence of a debris lag, the gully-LDM systems presented here seem to have their nearest terrestrial analogue in debris-covered glaciers or ice-cored moraines. In such systems, gullies form by melting of the interior ice in discrete zones where debris cover is thin. Once a point of collapse is initiated, exposed ice melts even more, and a positive feedback ensues, causing more failure. When sufficient debris builds up, failure halts [*Lukas et al.*, 2005]. This pattern of gully formation without complete destabilization and removal of the ice-cored substrate is similar to the observations of gullies in the LDM. This supports the hypothesis that gullies can be formed by melting of the LDM [*Schon et al.*, 2009b] and does not require an external reservoir (aquifer or snowmelt), as suggested by some authors [*Malin and Edgett*, 2000]. Alternately the presence of massive ice could act to trap carbon dioxide [*Vincendon et al.*, 2010], which could carve gullies by CO_2 sublimation processes [*Dundas et al.*, 2010; *Diniega et al.*, 2013; *Raack et al.*, 2014]. We think that this is unlikely for carving the chutes of these gullies given the erosive power required to incise into almost pure ice, as opposed to melting it.

Ice-rich deposits, tens of meters thick, on slopes are likely to undergo plastic deformation [*Milliken et al.*, 2003], and our sites do contain examples of flow (Figures 1a, 1e, and 3d). Hence, the pasted-on terrain could be a precursor to viscous flow features [*Milliken et al.*, 2003; *Souness et al.*, 2012], which are observed elsewhere in the midlatitude regions of Mars. If this is the case, the LDM exists within a glacial process domain in which precipitation, accumulation, and degradation find their analogues in cold and dry glacial landscapes on Earth.

Previous studies [*Jakosky and Carr*, 1985] proposed that the LDM was emplaced during periods of above average insolation at the poles (i.e., when Mars' axial tilt was $>30°$). During these periods, the most recent being ~0.35 Ma ago, water ice was redistributed from the poles to the midlatitudes [*Jakosky and Carr*, 1985]. Models suggest that a maximum of about 1 m of ice could have been emplaced during each of the 20 high-obliquity excursions which occurred during the last 2.1 Ma [*Mischna et al.*, 2003], yet the lack of internal layers within thick deposits of high-ice-content material in our study areas suggests that this material was emplaced during a single-obliquity excursion. Hence, in certain environments, a much greater thickness of LDM can be laid down in a single episode than was previously thought. This provides a possible explanation for the patchy distribution of other landforms thought to be emplaced by ice accumulation, such as glacier-like forms [*Souness et al.*, 2012].

Acknowledgments

We thank Jim Head for his constructive and useful reviews. We acknowledge the Leverhulme Trust for the support (grant RPG-397). Thanks to the HiRISE team for making their elevation data and images publically available. We are grateful for comments from David Rothery and Marion Massé. This is PSI contribution 619. The authors thank two anonymous reviewers for their helpful comments.

The Editor thanks two anonymous reviewers for their assistance in evaluating this paper.

References

Aston, A. H., S. J. Conway, and M. R. Balme (2011), Identifying Martian gully evolution, in *Martian Geomorphology*, vol. 356, edited by M. Balme et al., pp. 151–169, Geological Society, London, U. K.

Bremer, M., and O. Sass (2012), Combining airborne and terrestrial laser scanning for quantifying erosion and deposition by a debris flow event, *Geomorphology*, *138*(1), 49–60, doi:10.1016/j.geomorph.2011.08.024.

Byrne, S., et al. (2009), Distribution of mid-latitude ground ice on mars from new impact craters, *Science*, *325*(5948), 1674–1676, doi:10.1126/science.1175307.

Christensen, P. R. (2003), Formation of recent martian gullies through melting of extensive water-rich snow deposits, *Nature*, *422*(6927), 45–48.

Conway, S. J., and N. Mangold (2013), Evidence for Amazonian mid-latitude glaciation on Mars from impact crater asymmetry, *Icarus*, *225*(1), 413–423, doi:10.1016/j.icarus.2013.04.013.

Diniega, S., C. J. Hansen, J. N. McElwaine, C. H. Hugenholtz, C. M. Dundas, A. S. McEwen, and M. C. Bourke (2013), A new dry hypothesis for the formation of martian linear gullies, *Icarus*, *225*(1), 526–537, doi:10.1016/j.icarus.2013.04.006.

Dundas, C. M., A. S. McEwen, S. Diniega, S. Byrne, and S. Martinez-Alonso (2010), New and recent gully activity on Mars as seen by HiRISE, *Geophys. Res. Lett.*, *37*, L07202, doi:10.1029/2009gl041351.

Feldman, W. C., et al. (2004), Global distribution of near-surface hydrogen on Mars, *J. Geophys. Res.*, *109*, E09006, doi:10.1029/2003JE002160.

Fisher, D. A. (2005), A process to make massive ice in the martian regolith using long-term diffusion and thermal cracking, *Icarus*, *179*(2), 387–397, doi:10.1016/j.icarus.2005.07.024.

Head, J. W., J. F. Mustard, M. A. Kreslavsky, R. E. Milliken, and D. R. Marchant (2003), Recent ice ages on Mars, *Nature*, *426*(6968), 797–802, doi:10.1038/nature02114.

Jakosky, B. M., and M. H. Carr (1985), Possible precipitation of ice at low latitudes of Mars during periods of high obliquity, *Nature*, *315*(6020), 559–561, doi:10.1038/315559a0.

Kirk, R. L., et al. (2008), Ultrahigh resolution topographic mapping of Mars with MRO HiRISE stereo images: Meter-scale slopes of candidate Phoenix landing sites, *J. Geophys. Res.*, *113*, E00A24, doi:10.1029/2007JE003000.

Kreslavsky, M. A., and J. W. Head (2000), Kilometer-scale roughness of Mars: Results from MOLA data analysis, *J. Geophys. Res.*, *105*, 26,695–26,712, doi:10.1029/2000JE001259.

Kreslavsky, M. A., and J. W. Head (2002), Mars: Nature and evolution of young latitude-dependent water-ice-rich mantle, *Geophys. Res. Lett.*, *29*(15), 1719, doi:10.1029/2002GL015392.

Lachenbruch, A. H. (1961), Depth and spacing of tension cracks, *J. Geophys. Res.*, *66*(12), 4273–4292, doi:10.1029/JZ066i012p04273.

Levy, J. S., J. W. Head, and D. R. Marchant (2009a), Concentric crater fill in Utopia Planitia: History and interaction between glacial "brain terrain" and periglacial mantle processes, *Icarus*, *202*(2), 462–476, doi:10.1016/j.icarus.2009.02.018.

Levy, J. S., J. W. Head, D. R. Marchant, J. L. Dickson, and G. A. Morgan (2009b), Geologically recent gully-polygon relationships on Mars: Insights from the Antarctic dry valleys on the roles of permafrost, microclimates, and water sources for surface flow, *Icarus*, *201*(1), 113–126.

Levy, J. S., J. W. Head, and D. R. Marchant (2011), Gullies, polygons and mantles in Martian permafrost environments: Cold desert landforms and sedimentary processes during recent Martian geological history, *Geol. Soc. London Spec. Publ.*, *354*(1), 167–182, doi:10.1144/SP354.10.

Lukas, S., L. I. Nicholson, F. H. Ross, and O. Humlum (2005), Formation, meltout processes and landscape alteration of high-Arctic ice-cored moraines—Examples from Nordenskiold Land, central Spitsbergen, *Polar Geogr.*, *29*(3), 157–187, doi:10.1080/789610198.

Malin, M. C., and K. S. Edgett (2000), Evidence for recent groundwater seepage and surface runoff on Mars, *Science*, *288*(5475), 2330–2335, doi:10.1126/science.288.5475.2330.

Mellon, M. T., and B. M. Jakosky (1995), The distribution and behavior of Martian ground ice during past and present epochs, *J. Geophys. Res.*, *100*, 11,781–11,799, doi:10.1029/95JE01027.

Milliken, R. E., J. F. Mustard, and D. L. Goldsby (2003), Viscous flow features on the surface of Mars: Observations from high-resolution Mars Orbiter Camera (MOC) images, *J. Geophys. Res.*, *108*(E6), 5057, doi:10.1029/2002JE002005.

Mischna, M. A., M. I. Richardson, R. J. Wilson, and D. J. McCleese (2003), On the orbital forcing of Martian water and CO_2 cycles: A general circulation model study with simplified volatile schemes, *J. Geophys. Res.*, *108*(E6), 5062, doi:10.1029/2003JE002051.

Mustard, J. F., C. D. Cooper, and M. K. Rifkin (2001), Evidence for recent climate change on Mars from the identification of youthful near-surface ground ice, *Nature*, *412*(6845), 411–414, doi:10.1038/35086515.

Okubo, C. H. (2010), Structural geology of Amazonian-aged layered sedimentary deposits in southwest Candor Chasma, Mars, *Icarus*, *207*(1), 210–225, doi:10.1016/j.icarus.2009.11.012.

Raack, J., D. Reiss, and H. Hiesinger (2012), Gullies and their relationships to the dust-ice mantle in the northwestern Argyre Basin, Mars, *Icarus*, *219*, 129–141, doi:10.1016/j.icarus.2012.02.025.

Raack, J., D. Reiss, T. Appéré, M. Vincendon, O. Ruesch, and H. Hiesinger (2014), Present-day seasonal gully activity in a south polar pit (Sisyphi Cavi) on Mars, *Icarus*, doi:10.1016/j.icarus.2014.03.040, in press.

Robbins, S. J., and B. M. Hynek (2012), A new global database of Mars impact craters ≥1 km: 1. Database creation, properties, and parameters, *J. Geophys. Res.*, *117*, E05004, doi:10.1029/2011JE003966.

Schon, S. C., and J. W. Head (2011), Keys to gully formation processes on Mars: Relation to climate cycles and sources of meltwater, *Icarus*, *213*(1), 428–432, doi:10.1016/j.icarus.2011.02.020.

Schon, S. C., J. W. Head, and R. E. Milliken (2009a), A recent ice age on Mars: Evidence for climate oscillations from regional layering in mid-latitude mantling deposits, *Geophys. Res. Lett.*, *36*, L15202, doi:10.1029/2009GL038554.

Schon, S. C., J. W. Head, and C. I. Fassett (2009b), Unique chronostratigraphic marker in depositional fan stratigraphy on Mars: Evidence for ca. 1.25 Ma gully activity and surficial meltwater origin, *Geology*, *37*(3), 207–210, doi:10.1130/g25398a.1.

Schon, S. C., J. W. Head, and C. I. Fassett (2012), Recent high-latitude resurfacing by a climate-related latitude-dependent mantle: Constraining age of emplacement from counts of small craters, *Planet. Space Sci.*, *69*(1), 49–61, doi:10.1016/j.pss.2012.03.015.

Smith, P. H., et al. (2009), H_2O at the Phoenix Landing Site, *Science*, *325*(5936), 58–61, doi:10.1126/science.1172339.

Soare, R. J., A. Séjourné, G. Pearce, F. Costard, and G. R. Osinski (2011), The Tuktoyaktuk Coastlands of northern Canada: A possible "wet" periglacial analog of Utopia Planitia, Mars, *Geol. Soc. Am. Spec. Pap.*, *483*, 203–218, doi:10.1130/2011.2483(13).

Souness, C., B. Hubbard, R. E. Milliken, and D. Quincey (2012), An inventory and population-scale analysis of Martian glacier-like forms, *Icarus*, *217*(1), 243–255, doi:10.1016/j.icarus.2011.10.020.

Vincendon, M., J. Mustard, F. Forget, M. Kreslavsky, A. Spiga, S. Murchie, and J.-P. Bibring (2010), Near-tropical subsurface ice on Mars, *Geophys. Res. Lett.*, *37*, L01202, doi:10.1029/2009GL041426.